

Full 1-loop calculation of $\text{BR}(B_{s,d}^0 \rightarrow \ell\bar{\ell})$ in models beyond the MSSM with SARAH and SPheno

H. Dreiner^a, K. Nickel^a, W. Porod^b, F. Staub^a

^a*Bethe Center for Theoretical Physics & Physikalisches Institut der Universität Bonn, Nußallee 12, 53115 Bonn, Germany*

^b*Institut für Theoretische Physik und Astrophysik, Universität Würzburg, 97074 Würzburg, Germany*

Abstract

We present the possibility of calculating the quark flavor changing neutral current decays $B_s^0 \rightarrow \ell\bar{\ell}$ and $B_d^0 \rightarrow \ell\bar{\ell}$ for a large variety of supersymmetric models. For this purpose, the complete one-loop calculation has been implemented in a generic form in the *Mathematica* package SARAH. This information is used by SARAH to generate *Fortran* source code for SPheno for a numerical evaluation of these processes in a given model. We comment also on the possibility to use this setup for non-supersymmetric models.

1. Introduction

With the recent discovery of a bosonic resonance [1, 2] showing all the characteristics of the SM Higgs boson a long search might soon come to a successful end. In contrast there are no hints for a signal of supersymmetric (SUSY) particles or particles predicted by any other extension of the standard model (SM) [3–7]. Therefore, large areas of the parameter space of the simplest SUSY models are excluded. The allowed mass spectra as well as the best fit mass values to the data are pushed to higher and higher values [9]. This has lead to an increasing interest in the study of SUSY models which provide new features. For instance, models with broken R -parity [10, 11] or compressed spectra [12] might be able to hide much better at the LHC, while for other models high mass spectra are a much more natural feature than this is the case in the minimal-supersymmetric standard model (MSSM) [13].

However, bounds on the masses and couplings of beyond the SM (BSM) models follow not only from direct searches at colliders. New particles also have an impact on SM processes via virtual quantum corrections, leading in many instances to sizable deviations from the SM expectations. This holds in particular for the anomalous magnetic moment of the muon [14] and processes which are highly suppressed in the SM. The latter are mainly lepton flavor violating (LFV) or decays involving quark flavor changing neutral currents (qFCNC). While the prediction of LFV decays in the SM is many orders of magnitude below the experimental sensitivity [15], qFCNC is experimentally well established. For instance, the observed rate of $b \rightarrow s\gamma$ is in good agreement with the SM expectation and this observable has put for several years strong constraints on qFCNCs beyond the SM [16].

The experiments at the LHC have reached now a sensitivity to test also the SM prediction for $\text{BR}(B_s^0 \rightarrow \mu\bar{\mu})$ as well as $\text{BR}(B_d^0 \rightarrow \mu\bar{\mu})$ [17]

$$\text{BR}(B_s^0 \rightarrow \mu\bar{\mu})_{\text{SM}} = (3.23 \pm 0.27) \cdot 10^{-9}, \quad (1)$$

$$\text{BR}(B_d^0 \rightarrow \mu\bar{\mu})_{\text{SM}} = (1.07 \pm 0.10) \cdot 10^{-10}. \quad (2)$$

Email addresses: dreiner@uni-bonn.de (H. Dreiner), nickel@th.physik.uni-bonn.de (K. Nickel),
porod@physik.uni-wuerzburg.de (W. Porod), fnst Staub@th.physik.uni-bonn.de (F. Staub)

Using the measured finite width difference of the B mesons the time integrated branching ratio which should be compared to experiment is [18]

$$\text{BR}(B_s^0 \rightarrow \mu\bar{\mu})_{\text{theo}} = (3.56 \pm 0.18) \cdot 10^{-9}. \quad (3)$$

Recently, LHCb reported the first evidence for $B_s^0 \rightarrow \mu\bar{\mu}$. The observed rate [19]

$$\text{BR}(B_s^0 \rightarrow \mu\bar{\mu}) = (3.2_{-1.2}^{+1.5}) \times 10^{-9} \quad (4)$$

fits nicely to the SM prediction. For $\text{BR}(B_d^0 \rightarrow \mu\bar{\mu})$ the current upper bound: $9.4 \cdot 10^{-10}$ is already of the same order as the SM expectation.

This leads to new constraints for BSM models and each model has to be confronted with these measurements. So far, there exist several public tools which can calculate $\text{BR}(B_{s,d}^0 \rightarrow \ell\bar{\ell})$ as well as other observables in the context of the MSSM or partially also for the next-to-minimal supersymmetric standard model (NMSSM) [20]: `superiso` [21], `SUSY_Flavor` [22], `NMSSM-Tools` [23], `MicrOmegas` [24] or `SPheno` [25]. However, for more complicated SUSY models none of the available tools provides the possibility to calculate these decays easily. This gap is now closed by the interplay of the `Mathematica` package `SARAH` [26] and the spectrum generator `SPheno`. `SARAH` already has many SUSY models incorporated but allows also an easy and efficient implementation of new models. For all of these models `SARAH` can generate new modules for `SPheno` for a comprehensive numerical evaluation. This functionality is extended, as described in this paper, by a full 1-loop calculation of $B_{s,d}^0 \rightarrow \ell\bar{\ell}$.

The rest of the paper is organized as follows: in sec. 2 we recall briefly the analytical calculation for $\text{BR}(B_{s,d}^0 \rightarrow \ell\bar{\ell})$. In sec. 3 we discuss the implementation of this calculation in `SARAH` and `SPheno` before we conclude in sec. 4. The appendix contains more information about the calculation and generic results for the amplitudes.

2. Calculation of $\text{BR}(B_{s,d}^0 \rightarrow \ell\bar{\ell})$

In the SM this decay was first calculated in ref [27], in the analogous context of kaons. The higher order corrections were first presented in [28]; see also [29]. In the context of supersymmetry this was considered in [30]. See also the interesting correlation between $\text{BR}(B_s^0 \rightarrow \mu\bar{\mu})$ and $(g-2)_\mu$ [31].

We present briefly the main steps of the calculation of $\text{BR}(B_q^0 \rightarrow \ell_k\bar{\ell}_l)$ with $q = s, d$. We follow closely the notation of ref. [32]. The effective Hamiltonian can be parametrized by

$$\mathcal{H} = \frac{1}{16\pi^2} \sum_{X,Y=L,R} (C_{SXY} \mathcal{O}_{SXY} + C_{VXY} \mathcal{O}_{VXY} + C_{TX} \mathcal{O}_{TX}), \quad (5)$$

with the Wilson coefficients C_{SXY}, C_{VXY}, C_{TX} corresponding to the scalar, vector and tensor operators

$$\mathcal{O}_{SXY} = (\bar{q}_j P_X q_i)(\bar{\ell}_l P_Y \ell_k), \quad \mathcal{O}_{VXY} = (\bar{q}_j \gamma^\mu P_X q_i)(\bar{\ell}_l \gamma_\mu P_Y \ell_k), \quad \mathcal{O}_{TX} = (\bar{q}_j \sigma^{\mu\nu} P_X q_i)(\bar{\ell}_l \sigma_{\mu\nu} \ell_k). \quad (6)$$

P_L and P_R are the projection operators on left respectively right handed states. The expectation value of the axial vector matrix element is defined as

$$\langle 0 | \bar{b} \gamma^\mu \gamma^5 q | B_q^0(p) \rangle \equiv i p^\mu f_{B_q^0}. \quad (7)$$

Here, we introduced the meson decay constants $f_{B_q^0}$ which can be obtained from lattice QCD simulations [33]. The current values for B_s^0 and B_d^0 are given by [34]

$$f_{B_s^0} = (227 \pm 8) \text{ MeV}, \quad f_{B_d^0} = (190 \pm 8) \text{ MeV}. \quad (8)$$

Since the momentum p of the meson is the only four-vector available, the matrix element in eq. (7) can only depend on p^μ . The incoming momenta of the b antiquark and the s (or d) quark are p_1, p_2 respectively, where

$p = p_1 + p_2$. Contracting eq. (7) with p_μ and using the equations of motion $\bar{b}\not{p}_1 = -\bar{b}m_b$ and $\not{p}_2 q = m_q q$ leads to an expression for the pseudoscalar current

$$\langle 0 | \bar{b} \gamma^5 q | B_q^0(p) \rangle = -i \frac{M_{B_q^0}^2 f_{B_q^0}}{m_b + m_q}. \quad (9)$$

The vector and scalar currents vanish

$$\langle 0 | \bar{b} \gamma^\mu q | B_q^0(p) \rangle = \langle 0 | \bar{b} q | B_q^0(p) \rangle = 0. \quad (10)$$

From eqs. (7) and (9) we obtain

$$\langle 0 | \bar{b} \gamma^\mu P_{L/R} q | B_q^0(p) \rangle = \mp \frac{i}{2} p^\mu f_{B_q^0}, \quad \langle 0 | \bar{b} P_{L/R} q | B_q^0(p) \rangle = \pm \frac{i}{2} \frac{M_{B_q^0}^2 f_{B_q^0}}{m_b + m_q}. \quad (11)$$

In general, the matrix element \mathcal{M} is a function of the form factors F_S, F_P, F_V, F_A of the scalar, pseudoscalar, vector and axial-vector current and can be expressed by

$$(4\pi)^2 \mathcal{M} = F_S \bar{\ell} \ell + F_P \bar{\ell} \gamma^5 \ell + F_V p_\mu \bar{\ell} \gamma^\mu \ell + F_A p_\mu \bar{\ell} \gamma^\mu \gamma^5 \ell. \quad (12)$$

Note that there is no way of building an antisymmetric 2-tensor out of just one vector p^μ . The matrix element of the tensor operator \mathcal{O}_{TX} must therefore vanish. The form factors can be expressed by linear combinations of the Wilson coefficients of eq. (5)

$$F_S = \frac{i}{4} \frac{M_{B_q^0}^2 f_{B_q^0}}{m_b + m_q} (C_{SLL} + C_{SLR} - C_{SRR} - C_{SRL}), \quad (13)$$

$$F_P = \frac{i}{4} \frac{M_{B_q^0}^2 f_{B_q^0}}{m_b + m_q} (-C_{SLL} + C_{SLR} - C_{SRR} + C_{SRL}), \quad (14)$$

$$F_V = -\frac{i}{4} f_{B_q^0} (C_{VLL} + C_{VLR} - C_{VRR} - C_{VRL}), \quad (15)$$

$$F_A = -\frac{i}{4} f_{B_q^0} (-C_{VLL} + C_{VLR} - C_{VRR} + C_{VRL}). \quad (16)$$

The main task is to calculate the different Wilson coefficients for a given model. These Wilson coefficients receive at the 1-loop level contributions from various wave, penguin and box diagrams, see Figures B.4-B.10 in Appendix B. Furthermore, in some models these decays could also happen already at tree-level [35]. The amplitudes for all possible, generic diagrams which can contribute to the Wilson coefficients have been calculated with **FeynArts/FormCalc** [36] and the results are listed in Appendix B. This calculation has been performed in the $\overline{\text{DR}}$ scheme and 't Hooft gauge. How these results are used together with **SARAH** and **SPheno** to get numerical results will be discussed in the next section.

After the calculation of the form factors, the squared amplitude is

$$\begin{aligned} (4\pi)^4 |\mathcal{M}|^2 &= 2 |F_S|^2 \left(M_{B_q^0}^2 - (m_\ell + m_k)^2 \right) + 2 |F_P|^2 \left(M_{B_q^0}^2 - (m_\ell - m_k)^2 \right) \\ &\quad + 2 |F_V|^2 \left(M_{B_q^0}^2 (m_k - m_\ell)^2 - (m_k^2 - m_\ell^2)^2 \right) \\ &\quad + 2 |F_A|^2 \left(M_{B_q^0}^2 (m_k + m_\ell)^2 - (m_k^2 - m_\ell^2)^2 \right) \\ &\quad + 4 \Re(F_S F_V^*) (m_\ell - m_k) \left(M_{B_q^0}^2 + (m_k + m_\ell)^2 \right) \\ &\quad + 4 \Re(F_P F_A^*) (m_\ell + m_k) \left(M_{B_q^0}^2 - (m_k - m_\ell)^2 \right). \end{aligned} \quad (17)$$

Here, m_ℓ and m_k are the lepton masses. In the case $k = \ell$, this expression simplifies to

$$|\mathcal{M}|^2 = \frac{2}{(16\pi^2)^2} \left((M_{B_q^0}^2 - 4m_\ell^2) |F_S|^2 + M_{B_q^0}^2 |F_P|^2 + 2m_\ell F_A|^2 \right). \quad (18)$$

default SM input parameters				
$\alpha_{em}^{-1}(M_Z) = 127.93$	$\alpha_s(M_Z) = 0.1190$	$G_F = 1.16639 \cdot 10^{-5} \text{ GeV}^{-2}$	$\rho = 0.135$	$\eta = 0.349$
$m_t^{pole} = 172.90 \text{ GeV}$	$M_Z^{pole} = 91.1876 \text{ GeV}$	$m_b(m_b) = 4.2 \text{ GeV}$	$\lambda = 0.2257$	$A = 0.814$
derived parameters				
$m_t^{\overline{DR}} = 166.4 \text{ GeV}$	$ V_{tb}^* V_{ts} = 4.06 \cdot 10^{-2}$	$ V_{tb}^* V_{td} = 8.12 \cdot 10^{-3}$	$m_W = 80.3893$	$\sin^2 \Theta_W = 0.2228$

Table 1: SM input values and derived parameters by default used for the numerical evaluation of $B_{s,d}^0 \rightarrow \ell \bar{\ell}$ in **SPheno**.

Note, the result is independent of the form factor F_V in this limit. In the SM the leading 1-loop contributions proceed via the exchange of virtual gauge bosons. They are thus helicity suppressed. Furthermore, since these are flavor changing neutral currents, they are GIM suppressed. The diagrams involving virtual Higgs bosons are suppressed due to small Yukawa couplings. In BSM scenarios these suppressions can be absent.

The branching ratio is then given by

$$\text{BR}(B_q^0 \rightarrow \ell_k \bar{\ell}_l) = \frac{\tau_{B_q^0} |\mathcal{M}|^2}{16\pi M_{B_q^0}} \sqrt{1 - \left(\frac{m_k + m_l}{M_{B_q^0}}\right)^2} \sqrt{1 - \left(\frac{m_k - m_l}{M_{B_q^0}}\right)^2} \quad (19)$$

with $\tau_{B_q^0}$ as the life time of the mesons.

3. Automatized calculation of $B_{s,d}^0 \rightarrow \ell \bar{\ell}$

3.1. Implementation in SARAH and SPheno

SARAH is the first ‘spectrum-generator-generator’ on the market which means that it can generate Fortran source for **SPheno** to obtain a full-fledged spectrum generator for models beyond the MSSM. The main features of a **SPheno** module written by **SARAH** are a precise mass spectrum calculation based on 2-loop renormalization group equations (RGEs) and a full 1-loop calculation of the mass spectrum. Two-loop results known for the MSSM can be included. Furthermore, also the decays of SUSY and Higgs particles are calculated as well as observables like $\ell_i \rightarrow \ell_j \gamma$, $\ell_i \rightarrow 3\ell_j$, $b \rightarrow s \gamma$, $\delta \rho$, $(g-2)$, or electric dipole moments. For more information about the interplay between **SARAH** and **SPheno** we refer the interested reader to Ref. [37].

Here we extend the list of observables by $\text{BR}(B_s^0 \rightarrow \ell \bar{\ell})$ and $\text{BR}(B_d^0 \rightarrow \ell \bar{\ell})$. For this purpose, the generic tree-level and 1-loop amplitudes calculated with **FeynArts/FormCalc** given in Appendix B have been implemented in **SARAH**. When **SARAH** generates the output for **SPheno** it checks for all possible field combinations which can populate the generic diagrams in the given model. This information is then used to generate Fortran code for a numerical evaluation of all of these diagrams. The amplitudes are then combined to the Wilson coefficients which again are used to calculate the form factors eqs. (13)-(16). The branching ratio is finally calculated by using eq. (19). Note, the known 2-loop QCD corrections of Refs. [28, 29, 41] are not included in this calculation.

The Wilson coefficients for $B_{s,d}^0 \rightarrow \ell \bar{\ell}$ are calculated at a scale $Q = 160 \text{ GeV}$ by all modules generated by **SARAH**, as this is done by default by **SPheno** in the MSSM. Hence, as input parameters for the calculation the running SUSY masses and couplings at this scale obtained by a 2-loop RGE evaluation down from the SUSY scale are used. In the standard model gauge sector we use the running value of α_{em} , the on-shell Weinberg angle $\sin^2 \Theta_W^2 = 1 - \frac{m_W^2}{m_Z^2}$ with m_W calculated from $\alpha_{em}(M_Z)$, G_F and the Z mass. In addition, the CKM matrix calculated from the Wolfenstein parameters (λ, A, ρ, η) as well as the running quark masses enter the calculation. To obtain the running SM parameters at $Q = 160 \text{ GeV}$ we use 2-loop standard model RGEs of Ref. [42]. The default SM values as well as the derived parameters are given in Tab. 1. Note, even if CP violation is not switched on the calculation of the SUSY spectrum, always the phase of the CKM matrix is taken into account in these calculations. This is especially important for B_d^0 decays. All standard model parameters can be adjusted by using the corresponding standard blocks of the SUSY LesHouches Accord 2

Default hadronic parameters					
$m_{B_s^0} = 5.36677$ GeV	$f_{B_s^0} = 227(8)$ MeV	$\tau_{B_s^0} = 1.466(31)$ ps			
$m_{B_d^0} = 5.27958$ GeV	$f_{B_d^0} = 190(8)$ MeV	$\tau_{B_d^0} = 1.519(7)$ ps			

Table 2: Hadronic input values by default used for the numerical evaluation of $B_{s,d}^0 \rightarrow l\bar{l}$ in **SPheno**.

(SLHA2) [39]. Furthermore, the default input values for the hadronic parameters given in Table 2 are used. These can be changed in the Les Houches input accordingly to the Flavor Les Houches Accord (FLHA) [38] using the following blocks:

```
Block FLIFE          #
511  1.525E-12      # tau_Bd
531  1.472E-12      # tau_Bs
Block FMASS          #
511  5.27950  0  0  # M_Bd
531  5.3663  0  0  # M_Bs
Block FCONST         #
511  1  0.190  0  0  # f_Bd
531  1  0.227  0  0  # f_Bs
```

While **SPheno** includes the chiral resummation for the MSSM, this is not taken into account in the routines generated by **SARAH** because of its large model dependence.

3.2. Generating and running the source code

We describe briefly the main steps necessary to generate and run the **SPheno** code for a given model: after starting **Mathematica** and loading **SARAH** it is just necessary to evaluate the demanded model and call the function to generate the **SPheno** source code. For instance, to get a **SPheno** module for the B-L-SSM [43–45], use

```
<<[$SARAH-Directory]/SARAH.m;
Start["BLSSM"];
MakeSPheno[];
```

MakeSPheno[] calculates first all necessary information (*i.e.* vertices, mass matrices, tadpole equations, RGEs, self-energies) and then exports this information to Fortran code and writes all necessary auxiliary functions needed to compile the code together with **SPheno**. The entire output is saved in the directory

```
[$SARAH-Directory]/Output/BLSSM/EWSB/SPheno/
```

The content of this directory has to be copied into a new subdirectory of **SPheno** called **BLSSM** and afterwards the code can be compiled:

```
cp [$SARAH-Directory]/Output/BLSSM/EWSB/SPheno/* [$SPheno-Directory]/BLSSM/
cd [$SPheno-Directory]
make Model=BLSSM
```

This creates a new binary **SPhenoBLSSM** in the directory **bin** of **SPheno**. To run the spectrum calculation a file called **LesHouches.in.BLSSM** containing all input parameters in the Les Houches format has to be provided. **SARAH** writes also a template for such a file which has been copied with the other files to **/BLSSM**. This example can be evaluated via

```
./bin/SPhenoBLSSM BLSSM/LesHouches.in.BLSSM
```

and the output is written to `SPheno.spc.BLSSM`. This file contains all information like the masses, mass matrices, decay widths and branching ratios, and observables. For the $B_{s,d}^0 \rightarrow \ell\bar{\ell}$ decays the results are given twice for easier comparison: once for the full calculation and once including only the SM contributions. All results are written to the block `SPhenoLowEnergy` in the spectrum file using the following numbers:

4110	$\text{BR}^{SM}(B_d^0 \rightarrow e^+e^-)$	4111	$\text{BR}^{full}(B_d^0 \rightarrow e^+e^-)$
4220	$\text{BR}^{SM}(B_d^0 \rightarrow \mu^+\mu^-)$	4221	$\text{BR}^{full}(B_d^0 \rightarrow \mu^+\mu^-)$
4330	$\text{BR}^{SM}(B_d^0 \rightarrow \tau^+\tau^-)$	4331	$\text{BR}^{full}(B_d^0 \rightarrow \tau^+\tau^-)$
5110	$\text{BR}^{SM}(B_s^0 \rightarrow e^+e^-)$	5111	$\text{BR}^{full}(B_s^0 \rightarrow e^+e^-)$
5210	$\text{BR}^{SM}(B_s^0 \rightarrow \mu^+e^-)$	5211	$\text{BR}^{full}(B_s^0 \rightarrow \mu^+e^-)$
5220	$\text{BR}^{SM}(B_s^0 \rightarrow \mu^+\mu^-)$	5221	$\text{BR}^{full}(B_s^0 \rightarrow \mu^+\mu^-)$
5330	$\text{BR}^{SM}(B_s^0 \rightarrow \tau^+\tau^-)$	5331	$\text{BR}^{full}(B_s^0 \rightarrow \tau^+\tau^-)$

Note, we kept for completeness and as cross-check $\text{BR}^{SM}(B_s^0 \rightarrow \mu^+e^-)$ which has to vanish. The same steps can be repeated for any other model implemented in `SARAH`, or the `SUSY-Toolbox` scripts [37] can be used for an automatic implementation of new models in `SPheno` as well as in other tools based on the `SARAH` output.

3.3. Checks

We have performed several cross checks of the code generated by `SARAH`: the first, trivial check has been that we reproduce the known SM results and that those agree with the full calculation in the limit of heavy SUSY spectra. For the input parameters of Tab. 1 we obtain $\text{BR}(B_s^0 \rightarrow \mu^+\mu^-)^{SM} = 3.28 \cdot 10^{-9}$ and $\text{BR}(B_d^0 \rightarrow \mu^+\mu^-)^{SM} = 1.08 \cdot 10^{-10}$ which are in good agreement with eqs. (1)-(2). Secondly, as mentioned in the introduction there are several codes which calculate these decays for the MSSM or NMSSM. A detailed comparison of all of these codes is beyond the scope of the presentation here and will be presented elsewhere [40]. However, a few comments are in order: the code generated by `SARAH` as well as most other codes usually show the same behavior. There are differences in the numerical values calculated by the programs because of different values for the SM inputs. For instance, there is an especially strong dependence on the value of the electroweak mixing angle and, of course, of the hadronic parameters used in the calculation [17]. In addition, these processes are implemented with different accuracy in different tools: the treatment of NLO QCD corrections [41], chiral resummation [46], or SUSY box diagrams is not the same. Therefore, we depict in Fig. 1 a comparison between `SPheno` 3.2.1, `Superiso` 3.3 and `SPheno` by `SARAH` using the results normalized to the SM limit of each program.

It is also possible to perform a check of self-consistency: the leading-order contribution has to be finite which leads to non-trivial relations among the amplitudes for all wave and penguin diagrams are given in Appendix B.2 and Appendix B.3. Therefore, we can check these relations numerically by varying the renormalization scale used in all loop integrals. The dependence on this scale should cancel and the branching ratios should stay constant. This is shown in Figure 2: while single contributions can change by several orders the sum of all is numerically very stable.

3.4. Non-supersymmetric models

We have focused our discussion so far on SUSY models. However, even if `SARAH` is optimized for the study of SUSY models it is also able to handle non-SUSY models to some extent. The main drawback at the moment for non-SUSY models is that the RGEs can not be calculated because the results of Refs. [47, 48] which are used by `SARAH` are not valid in this case. However, all other calculations like the ones for the vertices, mass matrices and self-energies don't use SUSY properties and therefore apply to any model. Hence, it is also possible to generate `SPheno` code for these models which calculates $B_{s,d}^0 \rightarrow \ell\bar{\ell}$. The main difference in the calculation comes from the missing possibility to calculate the RGEs: the user has to provide numerical values for all parameters at the considered scale which then enter the calculation. We note that in order to fully support non-supersymmetric models with `SARAH` the calculation of the corresponding RGEs at 2-loop level will be included in `SARAH` in the future [49].

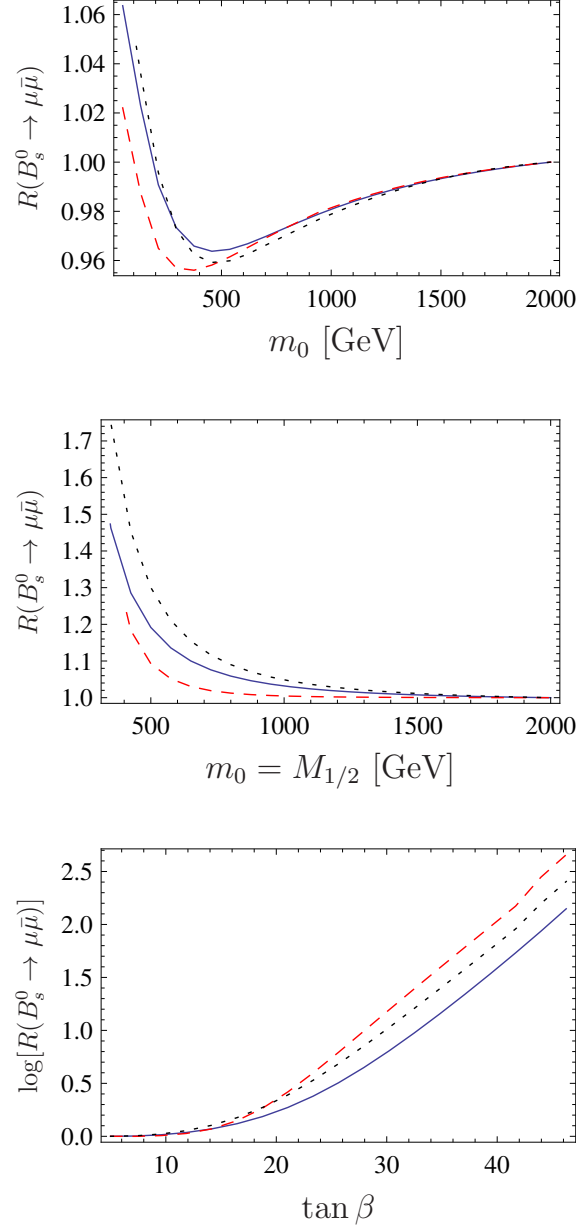


Figure 1: The top figure: $R = \text{BR}(B_s^0 \rightarrow \mu^+\mu^-)/\text{BR}(B_s^0 \rightarrow \mu^+\mu^-)_{SM}$ for the constrained MSSM and as function of m_0 . The other parameters were set to $M_{1/2} = 140$ GeV, $\tan \beta = 10$, $\mu > 0$. In the middle m_0 and $M_{1/2}$ were varied simultaneously, while $\tan \beta = 30$ was fixed. In the bottom figure we show $\log(R)$ as a function of $\tan \beta$, while $m_0 = M_{1/2} = 150$ GeV were kept fix. In all figures $A_0 = 0$ and $\mu > 0$ was used. The color code is as follows: **superiso** 3.3 (dotted black), **SPheno** 3.2.1 (dashed red) and **SPheno** by **SARAH** (solid blue).

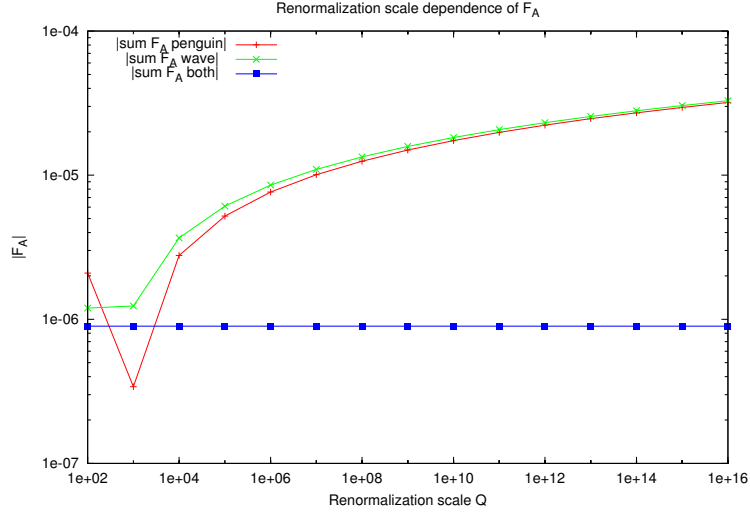


Figure 2: The figure shows $|\sum F_A|_{\text{penguin}}$ and $|\sum F_A|_{\text{wave}}$ as well as the sum of both $|\sum F_A|$. Penguin and wave contributions have opposite signs that interchange between $Q = 10^2 \text{ GeV}$ to $Q = 10^3 \text{ GeV}$.

4. Conclusion

We have presented a model independent implementation of the flavor violating decays $B_{s,d}^0 \rightarrow \ell \bar{\ell}$ in **SARAH** and **SPheno**. Our approach provides the possibility to generate source code which performs a full 1-loop calculation of these observables for any model which can be implemented in **SARAH**. Therefore, it takes care of the necessity to confront many BSM models in the future with the increasing constraints coming from the measurements of $B_{s,d}^0 \rightarrow \ell \bar{\ell}$ at the LHC.

Acknowledgements

W.P. thanks L. Hofer for discussions. This work has been supported by the Helmholtz alliance ‘Physics at the Terascale’ and W.P. in part by the DFG, project No. PO-1337/2-1. HKD acknowledges support from BMBF grant 00160200.

Appendix A. Conventions

Appendix A.1. Passarino-Veltman integrals

We use in the following the conventions of [50] for the Passarino-Veltman integrals. All Wilson coefficients appearing in the following can be expressed by the integrals

$$B_0(0, x, y) = \Delta + 1 + \ln\left(\frac{Q^2}{y}\right) + \frac{x}{x-y} \ln\left(\frac{y}{x}\right) \quad (\text{A.1})$$

$$\Delta = \frac{2}{4-D} - \gamma_E + \log 4\pi \quad (\text{A.2})$$

$$B_1(x, y, z) = \frac{1}{2}(z-y) \frac{B_0(x, y, z) - B_0(0, y, z)}{x} - \frac{1}{2}B_0(x, y, z) \quad (\text{A.3})$$

$$C_0(x, y, z) = \frac{1}{y-z} \left[\frac{y}{x-y} \log \frac{y}{x} - \frac{z}{x-z} \log \frac{z}{x} \right] \quad (\text{A.4})$$

$$C_{00}(x, y, z) = \frac{1}{4} \left(1 - \frac{1}{y-z} \left(\frac{x^2 \log x - y^2 \log y}{x-y} - \frac{x^2 \log x - z^2 \log z}{x-z} \right) \right) \quad (\text{A.5})$$

$$D_0(x, y, z, t) = \frac{C_0(x, y, z) - C_0(x, y, t)}{z-t} \quad (\text{A.6})$$

$$= - \left[\frac{y \log \frac{y}{x}}{(y-x)(y-z)(y-t)} + \frac{z \log \frac{z}{x}}{(z-x)(z-y)(z-t)} + \frac{t \log \frac{t}{x}}{(t-x)(t-y)(t-z)} \right]$$

$$D_{00}(x, y, z, t) = -\frac{1}{4} \left[\frac{y^2 \log \frac{y}{x}}{(y-x)(y-z)(y-t)} + \frac{z^2 \log \frac{z}{x}}{(z-x)(z-y)(z-t)} + \frac{t^2 \log \frac{t}{x}}{(t-x)(t-y)(t-z)} \right]$$

Note, the conventions of ref. [50] (Pierce, Bagger [PB]) are different than those presented in ref. [32] (Dedes, Rosiek, Tanedo [DRT]). The box integrals are related by

$$D_0 = D_0^{(\text{PB})} = -D_0^{(\text{DRT})}, \quad (\text{A.7a})$$

$$D_{00} = D_{27}^{(\text{PB})} = -\frac{1}{4}D_2^{(\text{DRT})}. \quad (\text{A.7b})$$

Appendix A.2. Massless limit of loop integrals

In some amplitudes (i.e. penguin diagrams ($a-b$), box diagram (v)) the following combinations of loop integrals appear:

$$I_1 = B_0(s, M_{F1}^2, M_{F2}^2) + M_S^2 C_0(s, 0, 0, M_{F2}^2, M_{F1}^2, M_S^2), \quad (\text{A.8})$$

$$I_2 = C_0(0, 0, 0, M_{F2}^2, M_{F1}^2, M_{V2}^2) + M_{V1}^2 D_0(M_{F2}^2, M_{F1}^2, M_{V1}^2, M_{V2}^2). \quad (\text{A.9})$$

The loop functions B_0, C_0, D_0 diverge for massless fermions (e.g. neutrinos in the MSSM) but the expressions I_1, I_2 are finite. However, this limit must be taken analytically in order to avoid numerical instabilities. In a generalized form and in the limit of zero external momenta, I_i can be expressed by

$$I_1(a, b, c) = B_0(0, a, b) + cC_0(0, 0, 0, a, b, c) \equiv B_0(0, a, b) + cC_0(a, b, c), \quad (\text{A.10})$$

$$I_2(a, b, c, d) = C_0(0, 0, 0, a, b, d) + cD_0(a, b, c, d) \equiv C_0(a, b, d) + cD_0(a, b, c, d). \quad (\text{A.11})$$

Using eqs. A.1, A.4, A.5 we obtain in the limit $a \rightarrow 0$

$$I_1(0, b, c) = B_0(0, 0, b) + cC_0(0, b, c) \quad (\text{A.12})$$

$$= \Delta + 1 - \log \frac{b}{Q^2} + c \frac{1}{b-c} \log \frac{c}{b} \quad (\text{A.13})$$

$$= \Delta + 1 + \log Q^2 + \frac{c}{b-c} \log c + \left(-1 - \frac{c}{b-c} \right) \log b \quad (\text{A.14})$$

The term proportional to $\log b$ vanishes in the limit $b \rightarrow 0$

$$I_1(0, 0, c) = \Delta + 1 - \log \frac{c}{Q^2} \quad (\text{A.15})$$

The same strategy works for I_2 :

$$I_2(0, b, c, d) = C_0(0, b, d) + cD_0(0, b, c, d) \quad (\text{A.16})$$

$$= \frac{1}{b-d} \log \frac{d}{b} + c \frac{C_0(0, b, c) - C_0(0, b, d)}{c-d} \quad (\text{A.17})$$

$$= \frac{1}{b-d} \log \frac{d}{b} + \frac{c}{c-d} \frac{1}{b-c} \log \frac{c}{b} - \frac{c}{c-d} \frac{1}{b-d} \log \frac{d}{b} \quad (\text{A.18})$$

$$= \frac{(c-d)(b-c) \log \frac{d}{b} + c(b-d) \log \frac{c}{b} - c(b-c) \log \frac{d}{b}}{(b-d)(c-d)(b-c)} \quad (\text{A.19})$$

The denominator of eq. (A.19) is finite for $b \rightarrow 0$ and in the numerator, the $\log b$ terms cancel each other:

$$((c-d)c + cd - c^2) \log b = 0. \quad (\text{A.20})$$

Hence, we end up with

$$I_2(0, 0, c, d) = \frac{-c(c-d) \log d - cd \log c + c^2 \log d}{cd(c-d)} = \frac{\log \frac{d}{c}}{c-d}. \quad (\text{A.21})$$

Appendix A.3. Parametrization of vertices

We are going to express the amplitude in the following in terms of generic vertices. For this purpose, we parametrize a vertex between two fermions and one vector or scalar respectively as

$$G_A \gamma_\mu P_L + G_B \gamma_\mu P_R, \quad (\text{A.22})$$

$$G_A P_L + G_B P_R. \quad (\text{A.23})$$

$P_{L,R} = \frac{1}{2}(1 \mp \gamma^5)$ are the polarization operators. In addition, for the vertex between three vector bosons and the one between one vector boson and two scalars the conventions are as follows

$$G_{VVV} \cdot (g_{\mu\nu}(k_2 - k_1)_\rho + g_{\nu\rho}(k_3 - k_2)_\mu + g_{\rho\mu}(k_1 - k_3)_\nu), \quad (\text{A.24})$$

$$G_{SSV} \cdot (k_1 - k_2)_\mu. \quad (\text{A.25})$$

Here, k_i are the (ingoing) momenta of the external particles.

Appendix B. Generic amplitudes

We present in the following the expressions for the generic amplitudes obtained with **FeynArts** and **FormCalc**. All coefficients that are not explicitly listed are zero. Furthermore, the Wilson coefficients are left-right symmetric, i.e.

$$C_{XRR} = C_{XLL}(L \leftrightarrow R), \quad C_{XRL} = C_{XLR}(L \leftrightarrow R), \quad (\text{B.1})$$

with $X = S, V$ and where $(L \leftrightarrow R)$ means that the coefficients of the left and right polarization part of each vertex have to be interchanged.

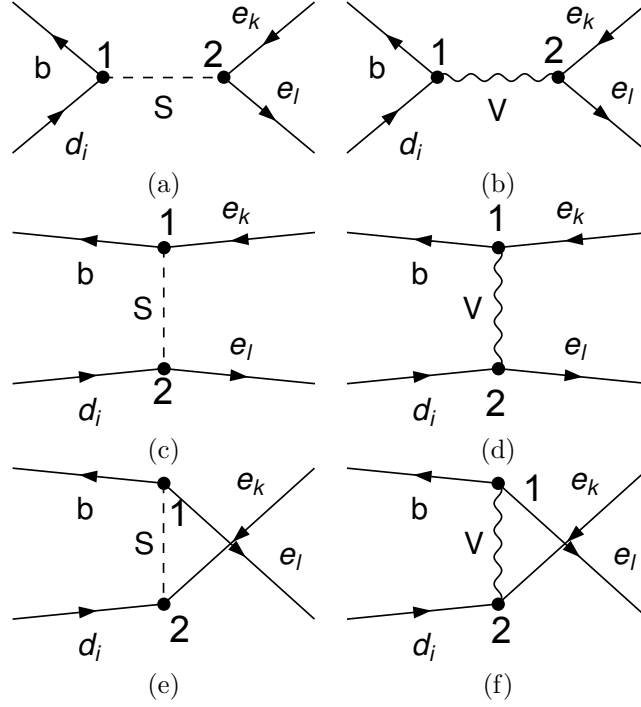


Figure B.3: Tree level diagrams with vertex numbering

Appendix B.1. Tree Level Contributions

Since in models beyond the MSSM it might be possible that $B_s^0 \rightarrow \ell \bar{\ell}$ is already possible at tree-level. This is for instance the case for trilinear R -parity violation [35]. The generic diagrams are given in Figure B.3. The chiral vertices are parametrized as in eqs. (A.22)-(A.23) with $A = 1, B = 2$ for vertex 1 and $A = 3, B = 4$ for vertex 2. Using these conventions, the corresponding contributions to the Wilson coefficients read

$$C_{SLL}^{(a)} = 16\pi^2 \frac{G_1 G_3}{M_S^2 - s}, \quad C_{SLR}^{(a)} = 16\pi^2 \frac{G_1 G_4}{M_S^2 - s} \quad (B.2)$$

$$C_{VLL}^{(b)} = 16\pi^2 \frac{-G_1 G_3}{M_V^2 - s}, \quad C_{VLR}^{(b)} = 16\pi^2 \frac{-G_1 G_4}{M_V^2 - s} \quad (B.3)$$

$$C_{SLL}^{(c)} = 16\pi^2 \frac{-G_1 G_3}{2(M_S^2 - t)}, \quad C_{VLR}^{(c)} = 16\pi^2 \frac{-G_2 G_3}{2(M_S^2 - t)} \quad (B.4)$$

$$C_{SLR}^{(d)} = 16\pi^2 \frac{2G_2 G_3}{M_V^2 - t}, \quad C_{VLL}^{(d)} = 16\pi^2 \frac{-G_1 G_3}{M_V^2 - t} \quad (B.5)$$

$$C_{SLL}^{(e)} = 16\pi^2 \frac{-G_1 G_3}{2(M_S^2 - u)}, \quad C_{VLL}^{(e)} = 16\pi^2 \frac{G_2 G_3}{2(M_S^2 - u)} \quad (B.6)$$

$$C_{SLR}^{(f)} = 16\pi^2 \frac{-2G_2 G_4}{M_V^2 - u}, \quad C_{VLR}^{(f)} = 16\pi^2 \frac{-G_1 G_4}{M_V^2 - u} \quad (B.7)$$

Here, s , t and u are the usual Mandelstam variables.

Appendix B.2. Wave Contributions

The generic wave diagrams are given in Figure B.4. The internal quark which attaches to the vector or scalar propagator has generation index n . Couplings that depend on n carry it as an additional index. The chiral vertices are parametrized as in eqs. (A.22)-(A.23) with $A = 1, B = 2$ for vertex 1, $A = 3, B = 4$ for

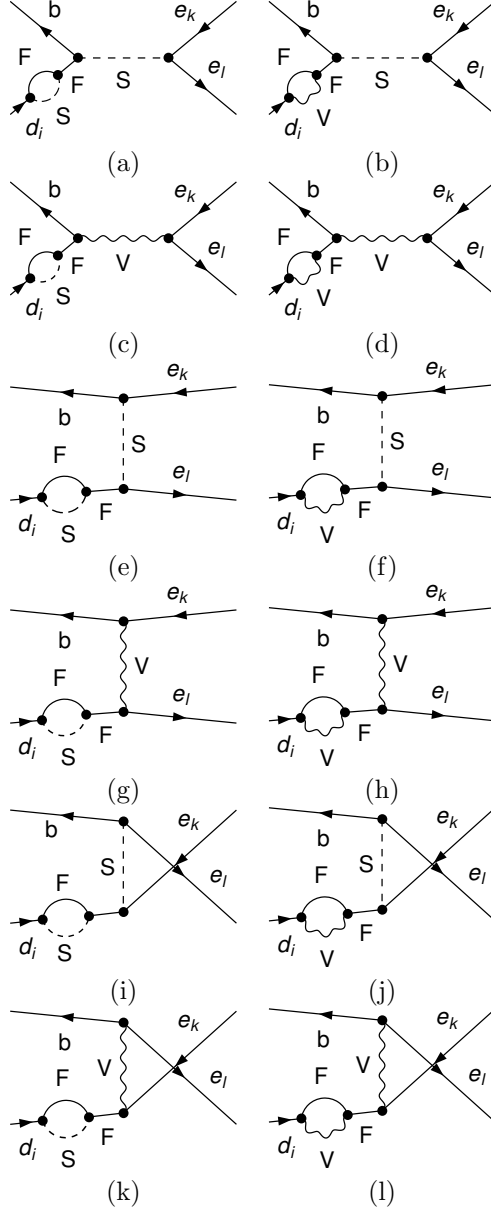


Figure B.4: Generic wave diagrams. For every diagram there is a crossed version, where the loop attaches to the other external quark.

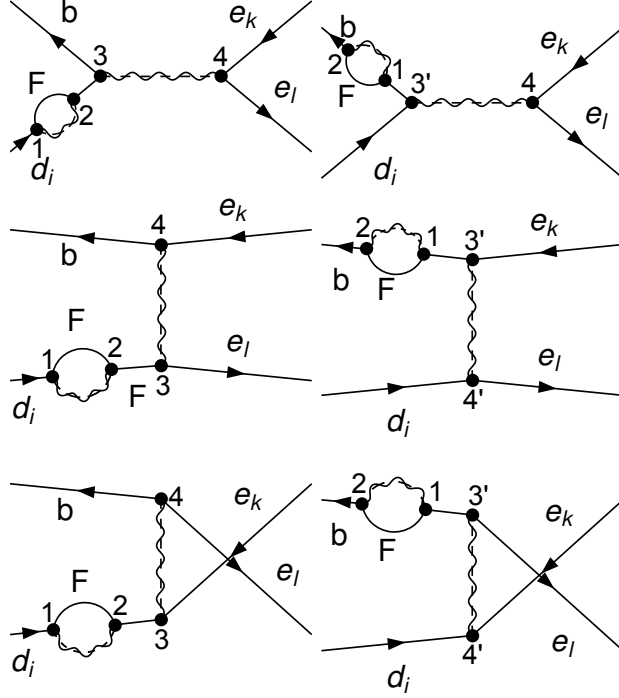


Figure B.5: Generic wave diagram vertex numbering

vertex 2, $A = 5, B = 6$ for vertex 3 and $A = 7, B = 8$ for vertex 4, see also Figure B.5 for the numbering of the vertices. If a vertex is labelled 3' for instance, the corresponding couplings are G'_5, G'_6 . Furthermore, we define the following abbreviations:

$$f_{S1} = \frac{1}{m_n^2 - m_i^2} \left(-M_F(G_1 G_{3n} m_n + G_2 G_{4n} m_i) B_0^{(i)} + (G_2 G_{3n} m_n m_i + G_1 G_{4n} m_i^2) B_1^{(i)} \right), \quad (\text{B.8})$$

$$f_{S2} = \frac{1}{m_j^2 - m_n^2} \left(M_F(G_{2n} G_4 m_j + G_{1n} G_3 m_n) B_0^{(j)} - (G_{2n} G_3 m_j^2 + G_{1n} G_4 m_j m_n) B_1^{(j)} \right), \quad (\text{B.9})$$

$$\tilde{f}_{S2} = \frac{1}{m_j^2 - m_n^2} \left(M_F(G_{1n} G_3 m_j + G_{2n} G_4 m_n) B_0^{(j)} - (G_{1n} G_4 m_j^2 + G_{2n} G_3 m_j m_n) B_1^{(j)} \right), \quad (\text{B.10})$$

$$f_{V1} = \frac{1}{m_n^2 - m_i^2} \left(2M_F(G_1 G_{4n} m_n + G_2 G_{3n} m_i) B_0^{(i)} + (G_2 G_{4n} m_n m_i + G_1 G_{3n} m_i^2) B_1^{(i)} \right), \quad (\text{B.11})$$

$$f_{V2} = \frac{1}{m_j^2 - m_n^2} \left(2M_F(G_{2n} G_3 m_j + G_{1n} G_4 m_n) B_0^{(j)} + (G_{2n} G_4 m_j^2 + G_{1n} G_3 m_j m_n) B_1^{(j)} \right), \quad (\text{B.12})$$

$$\tilde{f}_{V2} = \frac{1}{m_j^2 - m_n^2} \left(2M_F(G_{1n} G_4 m_j + G_{2n} G_3 m_n) B_0^{(j)} + (G_{1n} G_3 m_j^2 + G_{2n} G_4 m_j m_n) B_1^{(j)} \right). \quad (\text{B.13})$$

The m_i, m_j are the quark masses and $B_{0,1}^{(i)} = B_{0,1}(m_i^2, M_F^2, M_S^2)$ (or M_V^2 instead of M_S^2). m_n is the mass of the internal quark with generation index n . Couplings that involve the internal quark are also labelled with n (e.g. G_{3n}). Using these conventions, the contributions to the Wilson coefficients are

$$C_{SLL}^{(a)} = \frac{G_7}{M_{S0}^2 - s} (G_{5n} f_{S1} + G'_{5n} f_{S2}) \quad (\text{B.14})$$

$$C_{VLL}^{(c)} = \frac{G_7}{M_{V0}^2 - s} \left(-G_{5n} f_{S1} - G'_{5n} \tilde{f}_{S2} \right) \rightarrow \frac{G_7}{M_{V0}^2 - s} G_5 G_1 G_4 B_1(0, M_F, M_S) \quad (\text{B.15})$$

$$C_{SLL}^{(b)} = \frac{2G_7}{M_{S_0}^2 - s} (G_{5n}f_{V1} - G'_{5n}f_{V2}) \quad (\text{B.16})$$

$$C_{VLL}^{(d)} = \frac{2G_7}{M_{V_0}^2 - s} (-G_{5n}f_{V1} + G'_{5n}\tilde{f}_{V2}) \rightarrow \frac{2G_7}{M_{V_0}^2 - s} G_5 G_1 G_3 B_1(0, M_F, M_V) \quad (\text{B.17})$$

$$C_{SLL}^{(e)} = \frac{-1}{2(M_{S_0}^2 - t)} (G_{5n}G_7f_{S1} + G'_{5n}G'_7f_{S2}) \quad (\text{B.18})$$

$$C_{VLR}^{(e)} = \frac{-1}{2(M_{S_0}^2 - t)} (G_{5n}G_8f_{S1} + G'_{6n}G'_7\tilde{f}_{S2}) \quad (\text{B.19})$$

$$C_{SLR}^{(g)} = \frac{+2}{M_{V_0}^2 - t} (G_{5n}G_8f_{S1} + G'_{6n}G'_7f_{S2}) \quad (\text{B.20})$$

$$C_{VLL}^{(g)} = \frac{-1}{M_{V_0}^2 - t} (G_{5n}G_7f_{S1} + G'_{5n}G'_7\tilde{f}_{S2}) \quad (\text{B.21})$$

$$C_{SLL}^{(f)} = \frac{-1}{M_{S_0}^2 - t} (G_{5n}G_7f_{V1} - G'_{5n}G'_7f_{V2}) \quad (\text{B.22})$$

$$C_{VLR}^{(f)} = \frac{-1}{M_{S_0}^2 - t} (G_{5n}G_8f_{V1} - G'_{6n}G'_7\tilde{f}_{V2}) \quad (\text{B.23})$$

$$C_{SLR}^{(h)} = \frac{+4}{M_{V_0}^2 - t} (G_{5n}G_8f_{V1} - G'_{6n}G'_7f_{V2}) \quad (\text{B.24})$$

$$C_{VLL}^{(h)} = \frac{+2}{M_{V_0}^2 - t} (-G_{5n}G_7f_{V1} + G'_{5n}G'_7\tilde{f}_{V2}) \quad (\text{B.25})$$

$$C_{SLL}^{(i)} = \frac{-1}{2(M_{S_0}^2 - u)} (G_{5n}G_7f_{S1} + G'_{5n}G'_7f_{S2}) \quad (\text{B.26})$$

$$C_{VLL}^{(i)} = \frac{+1}{2(M_{S_0}^2 - u)} (G_{5n}G_8f_{S1} + G'_{6n}G'_7\tilde{f}_{S2}) \quad (\text{B.27})$$

$$C_{SLR}^{(k)} = \frac{-2}{M_{V_0}^2 - u} (G_{6n}G_8f_{S1} + G'_{6n}G'_8f_{S2}) \quad (\text{B.28})$$

$$C_{VLR}^{(k)} = \frac{-1}{M_{V_0}^2 - u} (G_{6n}G_7f_{S1} + G'_{5n}G'_8\tilde{f}_{S2}) \quad (\text{B.29})$$

$$C_{SLL}^{(j)} = \frac{-1}{M_{S_0}^2 - u} (G_{5n}G_7\tilde{f}_{V1} - G'_{5n}G'_7f_{V2}) \quad (\text{B.30})$$

$$C_{VLL}^{(j)} = \frac{-1}{M_{S_0}^2 - u} (-G_{5n}G_8\tilde{f}_{V1} + G'_{6n}G'_7\tilde{f}_{V2}) \quad (\text{B.31})$$

$$C_{SLR}^{(l)} = \frac{-4}{M_{V_0}^2 - u} (G_{6n}G_8\tilde{f}_{V1} - G'_{6n}G'_8f_{V2}) \quad (\text{B.32})$$

$$C_{VLR}^{(l)} = \frac{-2}{M_{V_0}^2 - u} (G_{6n}G_7\tilde{f}_{V1} - G'_{5n}G'_8\tilde{f}_{V2}) \quad (\text{B.33})$$

Appendix B.3. Penguin Contributions

Diagrams with scalar propagators have $C_{VXY} = 0$ and those with vector propagators have $C_{SXY} = 0$. The vertex number conventions are given in fig. B.6 and all possible diagrams are depicted in Figure B.7. The chiral vertices are parametrized as in eqs. (A.22)-(A.23) with $A = 1, B = 2$ for vertex 1, $A = 3, B = 4$ for vertex 2 and $A = 7, B = 8$ for vertex 4. Vertex 3 can be a chiral vertex, in this case $A = 5, B = 6$ is used. Otherwise, we will denote it with a index 5 and give as additional subscript the kind of vertex. The contributions to the Wilson coefficients from these diagrams read

$$C_{SLL}^{(a)} = \frac{1}{M_{S_0}^2 - s} G_1 G_3 G_7 \left(G_6 B_0^{(a,b)} + (G_5 M_{F1} M_{F2} + G_6 M_S^2) C_0^{(a,b)} \right) \quad (\text{B.34})$$

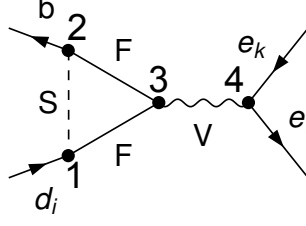


Figure B.6: Vertex number conventions for a representative penguin diagram

$$C_{SLR}^{(a)} = \frac{1}{M_{S0}^2 - s} G_1 G_3 G_8 \left(G_6 B_0^{(a,b)} + (G_5 M_{F1} M_{F2} + G_6 M_S^2) C_0^{(a,b)} \right) \quad (\text{B.35})$$

$$C_{VLL}^{(b)} = \frac{1}{M_{V0}^2 - s} G_1 G_4 G_7 \left(G_6 B_0^{(a,b)} + (-G_5 M_{F1} M_{F2} + G_6 M_S^2) C_0^{(a,b)} - 2G_6 C_{00}^{(a,b)} \right) \quad (\text{B.36})$$

$$C_{VLR}^{(b)} = \frac{1}{M_{V0}^2 - s} G_1 G_4 G_8 \left(G_6 B_0^{(a,b)} + (-G_5 M_{F1} M_{F2} + G_6 M_S^2) C_0^{(a,b)} - 2G_6 C_{00}^{(a,b)} \right) \quad (\text{B.37})$$

$$C_{SLL}^{(c)} = \frac{1}{M_{S0}^2 - s} G_1 G_3 G_{5,SSS} G_7 M_F C_0^{(c,d)} \quad (\text{B.38})$$

$$C_{SLR}^{(c)} = \frac{1}{M_{S0}^2 - s} G_1 G_3 G_{5,SSS} G_8 M_F C_0^{(c,d)} \quad (\text{B.39})$$

$$C_{VLL}^{(d)} = -\frac{2}{M_{V0}^2 - s} G_1 G_4 G_{5,SSV} G_7 C_{00}^{(c,d)} \quad (\text{B.40})$$

$$C_{VLR}^{(d)} = -\frac{2}{M_{V0}^2 - s} G_1 G_4 G_{5,SSV} G_8 C_{00}^{(c,d)} \quad (\text{B.41})$$

$$C_{SLL}^{(e)} = -\frac{4}{M_{S0}^2 - s} G_1 G_4 G_7 \left(G_5 B_0^{(e,f)} + (G_6 M_{F1} M_{F2} + G_5 M_V^2) C_0^{(e,f)} \right) \quad (\text{B.42})$$

$$C_{SLR}^{(e)} = -\frac{4}{M_{S0}^2 - s} G_1 G_4 G_8 \left(G_5 B_0^{(e,f)} + (G_6 M_{F1} M_{F2} + G_5 M_V^2) C_0^{(e,f)} \right) \quad (\text{B.43})$$

$$C_{VLL}^{(f)} = \frac{2}{M_{V0}^2 - s} G_1 G_3 G_7 \left(G_5 B_0^{(e,f)} + (-G_6 M_{F1} M_{F2} + G_5 M_V^2) C_0^{(e,f)} - 2G_5 C_{00}^{(e,f)} \right) \quad (\text{B.44})$$

$$C_{VLR}^{(f)} = \frac{2}{M_{V0}^2 - s} G_1 G_3 G_8 \left(G_5 B_0^{(e,f)} + (-G_6 M_{F1} M_{F2} + G_5 M_V^2) C_0^{(e,f)} - 2G_5 C_{00}^{(e,f)} \right) \quad (\text{B.45})$$

$$C_{SLL}^{(g)} = \frac{4}{M_{S0}^2 - s} G_1 G_4 G_{5,SVV} G_7 M_F C_0^{(g,h)} \quad (\text{B.46})$$

$$C_{SLR}^{(g)} = \frac{4}{M_{S0}^2 - s} G_1 G_4 G_{5,SVV} G_8 M_F C_0^{(g,h)} \quad (\text{B.47})$$

$$C_{VLL}^{(h)} = -\frac{2}{M_{V0}^2 - s} G_1 G_3 G_{5,VVV} G_7 \left(B_0^{(g,h)} + M_F^2 C_0^{(g,h)} + 2C_{00}^{(g,h)} \right) \quad (\text{B.48})$$

$$C_{VLR}^{(h)} = -\frac{2}{M_{V0}^2 - s} G_1 G_3 G_{5,VVV} G_8 \left(B_0^{(g,h)} + M_F^2 C_0^{(g,h)} + 2C_{00}^{(g,h)} \right) \quad (\text{B.49})$$

$$C_{SLL}^{(i)} = \frac{1}{M_{S0}^2 - s} G_1 G_3 G_{5,SSV} G_7 \left(B_0^{(i-l)} + M_F^2 C_0^{(i-l)} \right) \quad (\text{B.50})$$

$$C_{SLR}^{(i)} = \frac{1}{M_{S0}^2 - s} G_1 G_3 G_{5,SSV} G_8 \left(B_0^{(i-l)} + M_F^2 C_0^{(i-l)} \right) \quad (\text{B.51})$$

$$C_{SLL}^{(k)} = -\frac{1}{M_{S0}^2 - s} G_1 G_4 G_{5,SSV} G_7 \left(B_0^{(i-l)} + M_F^2 C_0^{(i-l)} \right) \quad (\text{B.52})$$

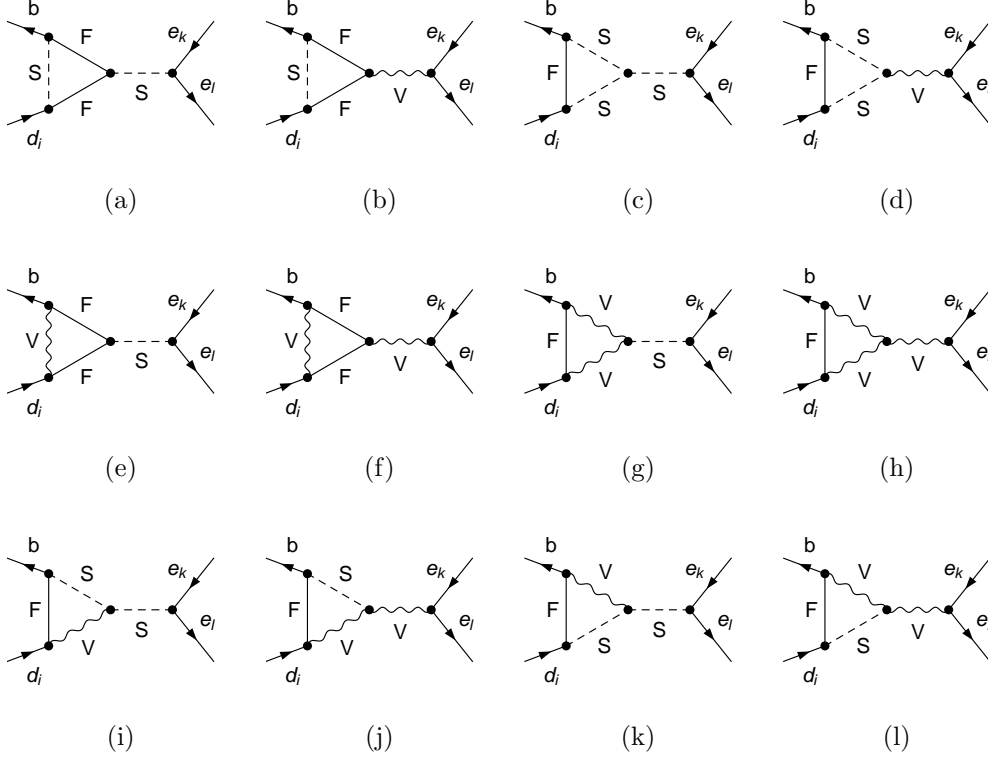


Figure B.7: Generic penguin diagrams

$$C_{SLR}^{(k)} = -\frac{1}{M_{S0}^2 - s} G_1 G_4 G_{5,SSV} G_8 \left(B_0^{(i-l)} + M_F^2 C_0^{(i-l)} \right) \quad (\text{B.53})$$

$$C_{VLL}^{(j)} = \frac{1}{M_{V0}^2 - s} G_1 G_4 G_{5,SVV} G_7 M_F C_0^{(i-l)} \quad (\text{B.54})$$

$$C_{VLR}^{(j)} = \frac{1}{M_{V0}^2 - s} G_1 G_4 G_{5,SVV} G_8 M_F C_0^{(i-l)} \quad (\text{B.55})$$

$$C_{VLL}^{(l)} = \frac{1}{M_{V0}^2 - s} G_1 G_3 G_{5,SVV} G_7 M_F C_0^{(i-l)} \quad (\text{B.56})$$

$$C_{VLR}^{(l)} = \frac{1}{M_{V0}^2 - s} G_1 G_3 G_{5,SVV} G_8 M_F C_0^{(i-l)} \quad (\text{B.57})$$

Here, the arguments of the Passarino-Veltman integrals are as follows, with $s = M_{B_q^0}^2$:

$$C_X^{(a,b)} = C_X(s, 0, 0, M_{F2}^2, M_{F1}^2, M_S^2) \quad B_X^{(a,b)} = B_X(s, M_{F1}^2, M_{F2}^2) \quad (\text{B.58})$$

$$C_X^{(c,d)} = C_X(0, s, 0, M_F^2, M_{S1}^2, M_{S2}^2) \quad (\text{B.59})$$

$$C_X^{(e,f)} = C_X(s, 0, 0, M_{F2}^2, M_{F1}^2, M_V^2) \quad B_X^{(e,f)} = B_X(s, M_{F1}^2, M_{F2}^2) \quad (\text{B.60})$$

$$C_X^{(g,h)} = C_X(0, s, 0, M_F^2, M_{V1}^2, M_{V2}^2) \quad B_X^{(g,h)} = B_X(s, M_{V1}^2, M_{V2}^2) \quad (\text{B.61})$$

$$C_X^{(i-l)} = C_X(0, s, 0, M_F^2, M_S^2, M_V^2) \quad B_X^{(i-l)} = B_X(s, M_S^2, M_V^2) \quad (\text{B.62})$$

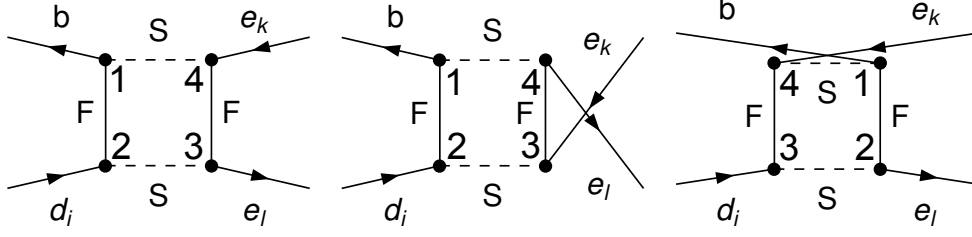


Figure B.8: Vertex number conventions for a set of representative box diagrams

Appendix B.4. Box Contributions

The vertex number conventions for boxes are shown in figs. B.8, while all possible generic diagrams are given in Figures B.9 and B.10. All vertices are chiral and they are parametrized as in eqs. (A.22)-(A.23) with $A = 1, B = 2$ for vertex 1, $A = 3, B = 4$ for vertex 2, $A = 5, B = 6$ for vertex 3 and $A = 7, B = 8$ for vertex 4. If there are two particles of equal type in a loop (say, two fermions), the one between vertices 1 and 2 (2 or 3) will be labelled $F1$ and the other one will be $F2$. The contributions to the different Wilson coefficients read

$$C_{SLL}^{(a)} = -G_1 G_3 G_5 G_7 M_{F1} M_{F2} \cdot D_0^{(a-c)} \quad (B.63)$$

$$C_{SLR}^{(a)} = -G_1 G_3 G_6 G_8 M_{F1} M_{F2} \cdot D_0^{(a-c)} \quad (B.64)$$

$$C_{VLL}^{(a)} = -G_2 G_3 G_6 G_7 \cdot D_{00}^{(a-c)} \quad (B.65)$$

$$C_{VLR}^{(a)} = -G_2 G_3 G_5 G_8 \cdot D_{00}^{(a-c)} \quad (B.66)$$

$$C_{SLL}^{(b)} = -G_1 G_3 G_5 G_7 M_{F1} M_{F2} \cdot D_0^{(a-c)} \quad (B.67)$$

$$C_{SLR}^{(b)} = -G_1 G_3 G_6 G_8 M_{F1} M_{F2} \cdot D_0^{(a-c)} \quad (B.68)$$

$$C_{VLL}^{(b)} = G_2 G_3 G_5 G_8 \cdot D_{00}^{(a-c)} \quad (B.69)$$

$$C_{VLR}^{(b)} = G_2 G_3 G_6 G_7 \cdot D_{00}^{(a-c)} \quad (B.70)$$

$$C_{SLL}^{(c)} = \frac{1}{2} G_1 G_3 G_5 G_7 M_{F1} M_{F2} D_0^{(a-c)} \quad (B.71)$$

$$C_{SLR}^{(c)} = -2 G_1 G_4 G_5 G_8 D_{00}^{(a-c)} \quad (B.72)$$

$$C_{VLL}^{(c)} = -\frac{1}{2} G_2 G_4 G_5 G_7 M_{F1} M_{F2} D_0^{(a-c)} \quad (B.73)$$

$$C_{VLR}^{(c)} = -G_2 G_3 G_5 G_8 D_{00}^{(a-c)} \quad (B.74)$$

$$C_{SLL}^{(d)} = \frac{1}{2} G_1 G_3 G_5 G_7 M_1 M_2 \cdot D_0^{(d-f)} \quad (B.75)$$

$$C_{SLR}^{(d)} = 2 G_1 G_3 G_6 G_8 \cdot D_{00}^{(d-f)} \quad (B.76)$$

$$C_{VLL}^{(d)} = -G_2 G_3 G_6 G_7 \cdot D_{00}^{(d-f)} \quad (B.77)$$

$$C_{VLR}^{(d)} = \frac{1}{2} G_2 G_3 G_5 G_8 M_1 M_2 \cdot D_0^{(d-f)} \quad (B.78)$$

$$C_{SLL}^{(e)} = \frac{1}{2} G_1 G_3 G_5 G_7 M_{F1} M_{F2} \cdot D_0^{(d-f)} \quad (B.79)$$

$$C_{SLR}^{(e)} = 2 G_1 G_3 G_6 G_8 \cdot D_{00}^{(d-f)} \quad (B.80)$$

$$C_{VLL}^{(e)} = -\frac{1}{2} G_2 G_3 G_5 G_8 M_{F1} M_{F2} \cdot D_0^{(d-f)} \quad (B.81)$$

$$C_{VLR}^{(e)} = G_2 G_3 G_6 G_7 \cdot D_{00}^{(d-f)} \quad (B.82)$$

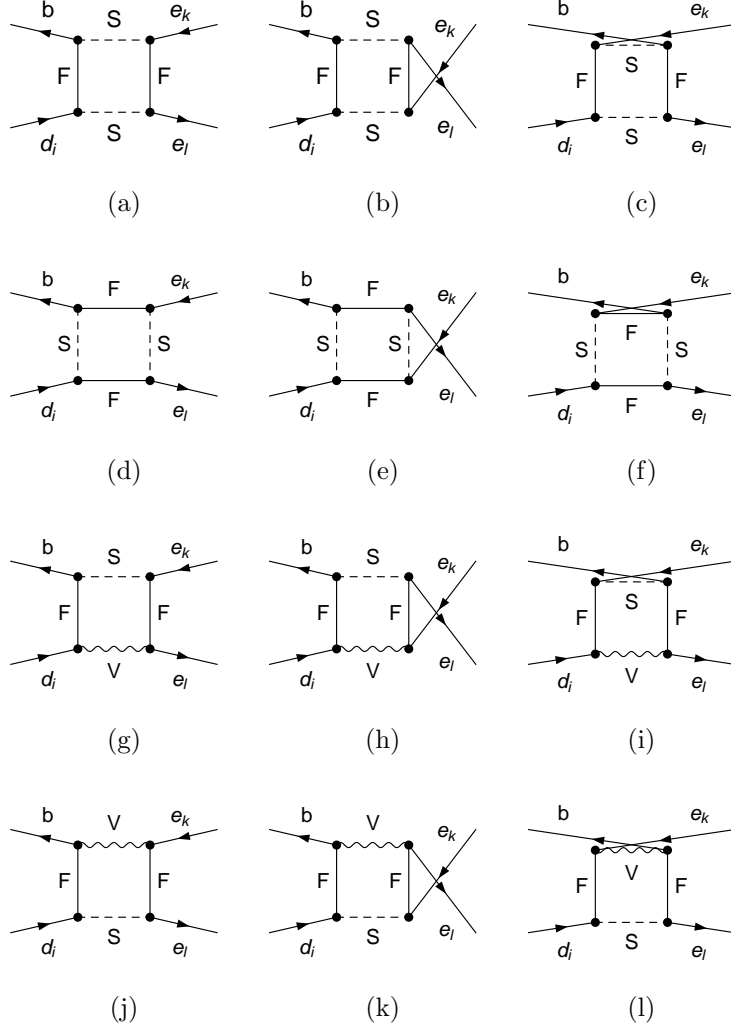


Figure B.9: Generic box diagrams I

$$C_{SLL}^{(f)} = \frac{1}{2} G_1 G_3 G_5 G_7 M_{F1} M_{F2} D_0^{(d-f)} \quad (\text{B.83})$$

$$C_{SLR}^{(f)} = -2 G_1 G_4 G_5 G_8 D_{00}^{(d-f)} \quad (\text{B.84})$$

$$C_{VLL}^{(f)} = G_2 G_4 G_5 G_7 D_{00}^{(d-f)} \quad (\text{B.85})$$

$$C_{VLR}^{(f)} = \frac{1}{2} G_2 G_3 G_5 G_8 M_{F1} M_{F2} D_0^{(d-f)} \quad (\text{B.86})$$

$$C_{SLL}^{(g)} = 2 G_1 G_3 G_6 G_7 \left(C_0^{(g-i)} + M_{F1}^2 D_0^{(g-i)} - 2 D_{00}^{(g-i)} \right) \quad (\text{B.87})$$

$$C_{SLR}^{(g)} = 2 G_1 G_3 G_5 G_8 \left(C_0^{(g-i)} + M_{F1}^2 D_0^{(g-i)} - 2 D_{00}^{(g-i)} \right) \quad (\text{B.88})$$

$$C_{VLL}^{(g)} = G_2 G_3 G_5 G_7 M_{F1} M_{F2} D_0^{(g-i)} \quad (\text{B.89})$$

$$C_{VLR}^{(g)} = G_2 G_3 G_6 G_8 M_{F1} M_{F2} D_0^{(g-i)} \quad (\text{B.90})$$

$$C_{SLL}^{(h)} = -4 G_1 G_3 G_5 G_7 D_{00}^{(g-i)} \quad (\text{B.91})$$

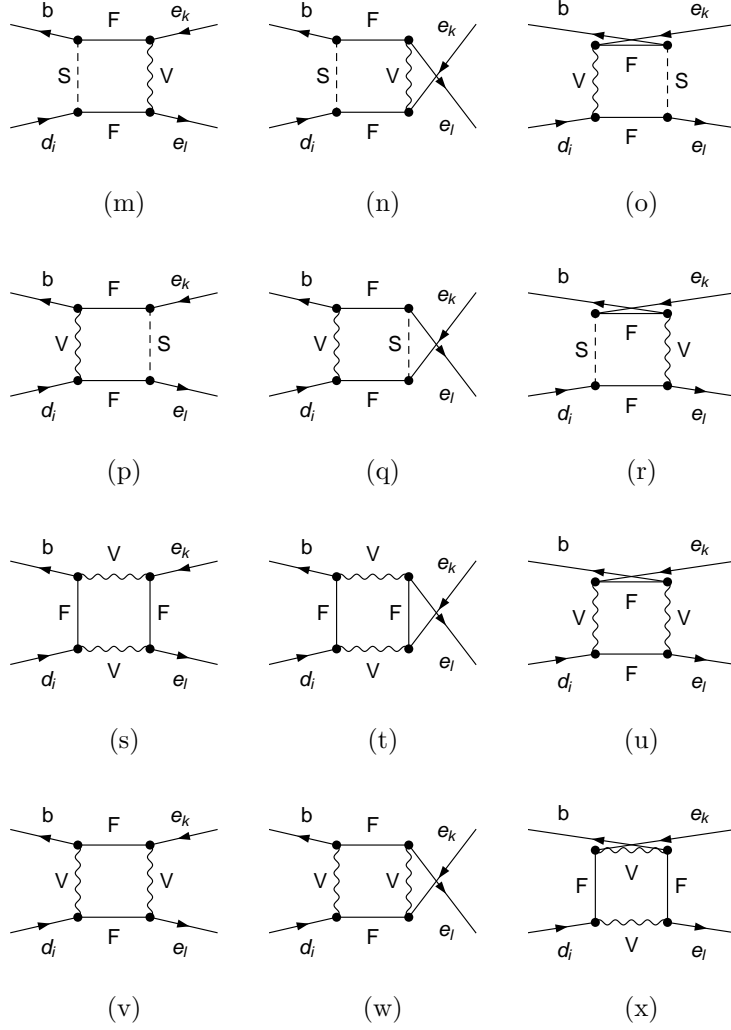


Figure B.10: Generic box diagrams II

$$C_{SLR}^{(h)} = -4G_1G_3G_6G_8D_{00}^{(g-i)} \quad (\text{B.92})$$

$$C_{VLL}^{(h)} = G_2G_3G_5G_8M_{F1}M_{F2}D_0^{(g-i)} \quad (\text{B.93})$$

$$C_{VLR}^{(g)} = G_2G_3G_6G_7M_{F1}M_{F2}D_0^{(g-i)} \quad (\text{B.94})$$

$$C_{SLL}^{(i)} = -G_1G_3G_5G_7 \left(C_0^{(g-i)} + M_S^2 D_0^{(g-i)} - 8D_{00}^{(g-i)} \right) \quad (\text{B.95})$$

$$C_{SLR}^{(i)} = 2G_1G_3G_5G_8M_{F1}M_{F2}D_0^{(g-i)} \quad (\text{B.96})$$

$$C_{VLL}^{(i)} = G_2G_3G_5G_7 \left(C_0^{(g-i)} + M_S^2 D_0^{(g-i)} - 2D_{00}^{(g-i)} \right) \quad (\text{B.97})$$

$$C_{VLR}^{(i)} = G_2G_4G_5G_8M_{F1}M_{F2}D_0^{(g-i)} \quad (\text{B.98})$$

$$C_{SLL}^{(j)} = 2G_2G_3G_5G_7 \left(C_0^{(j-l)} + M_{F1}^2 D_0^{(j-l)} - 2D_{00}^{(j-l)} \right) \quad (\text{B.99})$$

$$C_{SLR}^{(j)} = 2G_2G_3G_6G_8 \left(C_0^{(j-l)} + M_{F1}^2 D_0^{(j-l)} - 2D_{00}^{(j-l)} \right) \quad (\text{B.100})$$

$$C_{VLL}^{(j)} = G_1 G_3 G_6 G_7 M_{F1} M_{F2} D_0^{(j-l)} \quad (\text{B.101})$$

$$C_{VLR}^{(j)} = G_1 G_3 G_5 G_8 M_{F1} M_{F2} D_0^{(j-l)} \quad (\text{B.102})$$

$$C_{SLL}^{(k)} = -4 G_2 G_3 G_5 G_8 D_{00}^{(j-l)} \quad (\text{B.103})$$

$$C_{SLR}^{(k)} = -4 G_2 G_3 G_6 G_7 D_{00}^{(j-l)} \quad (\text{B.104})$$

$$C_{VLL}^{(k)} = G_1 G_3 G_5 G_7 M_{F1} M_{F2} D_0^{(j-l)} \quad (\text{B.105})$$

$$C_{VLR}^{(k)} = G_1 G_3 G_6 G_8 M_{F1} M_{F2} D_0^{(j-l)} \quad (\text{B.106})$$

$$C_{SLL}^{(l)} = -G_1 G_3 G_5 G_8 (C_0^{(j-l)} + M_V^2 D_0^{(j-l)} - 8 D_{00}^{(j-l)}) \quad (\text{B.107})$$

$$C_{SLR}^{(l)} = 2 G_1 G_4 G_5 G_7 M_{F1} M_{F2} D_0^{(j-l)} \quad (\text{B.108})$$

$$C_{VLL}^{(l)} = G_2 G_4 G_5 G_8 (C_0^{(j-l)} + M_V^2 D_0^{(j-l)} - 2 D_{00}^{(j-l)}) \quad (\text{B.109})$$

$$C_{VLR}^{(l)} = G_2 G_3 G_5 G_7 M_{F1} M_{F2} D_0^{(j-l)} \quad (\text{B.110})$$

$$C_{SLL}^{(m)} = -G_1 G_3 G_6 G_7 \left(C_0^{(m-o)} + M_S^2 D_0^{(m-o)} - \frac{1}{4} (13 G_1 G_3 G_6 G_7 + 3 G_2 G_4 G_5 G_8) D_{00}^{(m-o)} \right) \quad (\text{B.111})$$

$$C_{SLR}^{(m)} = -2 G_1 G_3 G_5 G_8 M_{F1} M_{F2} D_0^{(m-o)} \quad (\text{B.112})$$

$$C_{VLL}^{(m)} = G_2 G_3 G_5 G_7 M_{F1} M_{F2} D_0^{(m-o)} \quad (\text{B.113})$$

$$C_{VLR}^{(m)} = -G_2 G_3 G_6 G_8 \left(C_0^{(m-o)} + M_S^2 D_0^{(m-o)} - 2 D_{00}^{(m-o)} \right) \quad (\text{B.114})$$

$$C_{SLL}^{(n)} = 8 G_1 G_3 G_6 G_8 D_{00}^{(m-o)} \quad (\text{B.115})$$

$$C_{SLR}^{(n)} = 2 G_1 G_3 G_5 G_7 M_{F1} M_{F2} D_0^{(m-o)} \quad (\text{B.116})$$

$$C_{VLL}^{(n)} = -2 G_2 G_3 G_6 G_7 D_{00}^{(m-o)} \quad (\text{B.117})$$

$$C_{VLR}^{(n)} = G_2 G_3 G_5 G_8 M_{F1} M_{F2} D_0^{(m-o)} \quad (\text{B.118})$$

$$C_{SLL}^{(o)} = -\frac{1}{4} (13 G_1 G_3 G_5 G_7 + 3 G_2 G_4 G_6 G_8) D_{00}^{(m-o)} \quad (\text{B.119})$$

$$C_{SLR}^{(o)} = -2 G_1 G_4 G_5 G_8 M_{F1} M_{F2} D_0^{(m-o)} \quad (\text{B.120})$$

$$C_{VLL}^{(o)} = G_2 G_4 G_5 G_7 M_{F1} M_{F2} D_0^{(m-o)} \quad (\text{B.121})$$

$$C_{VLR}^{(o)} = 2 G_2 G_3 G_5 G_8 D_{00}^{(m-o)} \quad (\text{B.122})$$

$$C_{SLL}^{(p)} = -G_2 G_3 G_5 G_7 \left(C_0^{(p-r)} + M_V^2 D_0^{(p-r)} - \frac{1}{4} (13 G_2 G_3 G_5 G_7 + 3 G_1 G_4 G_6 G_8) D_{00}^{(p-r)} \right) \quad (\text{B.123})$$

$$C_{SLR}^{(p)} = -2 G_2 G_3 G_6 G_8 M_{F1} M_{F2} D_0^{(p-r)} \quad (\text{B.124})$$

$$C_{VLL}^{(p)} = G_1 G_3 G_6 G_7 M_{F1} M_{F2} D_0^{(p-r)} \quad (\text{B.125})$$

$$C_{VLR}^{(p)} = -G_1 G_3 G_5 G_8 \left(C_0^{(p-r)} + M_V^2 D_0^{(p-r)} - 2 D_{00}^{(p-r)} \right) \quad (\text{B.126})$$

$$C_{SLL}^{(r)} = 8 G_1 G_3 G_5 G_7 D_{00}^{(p-r)} \quad (\text{B.127})$$

$$C_{SLR}^{(q)} = 2 G_1 G_3 G_6 G_8 M_{F1} M_{F2} D_0^{(p-r)} \quad (\text{B.128})$$

$$C_{VLL}^{(q)} = -2 G_2 G_3 G_5 G_8 D_{00}^{(p-r)} \quad (\text{B.129})$$

$$C_{VLR}^{(q)} = G_2 G_3 G_6 G_7 M_{F1} M_{F2} D_0^{(p-r)} \quad (\text{B.130})$$

$$C_{SLL}^{(r)} = -\frac{1}{4} (13 G_2 G_4 G_5 G_7 + 3 G_1 G_3 G_6 G_8) D_{00}^{(p-r)} \quad (\text{B.131})$$

$$C_{SLR}^{(r)} = -2 G_2 G_3 G_5 G_8 M_{F1} M_{F2} D_0^{(p-r)} + \frac{3}{4} (G_2 G_4 G_5 G_7 - G_1 G_3 G_6 G_8) D_{00}^{(p-r)} \quad (\text{B.132})$$

$$C_{VLL}^{(r)} = G_1 G_3 G_5 G_7 M_{F1} M_{F2} D_0^{(p-r)} \quad (B.133)$$

$$C_{VLR}^{(r)} = 2G_1 G_4 G_5 G_8 D_0^{(p-r)} \quad (B.134)$$

$$C_{SLL}^{(s)} = -4G_2 G_3 G_6 G_7 M_{F1} M_{F2} D_0^{(s-u)} \quad (B.135)$$

$$C_{SLR}^{(s)} = -4G_2 G_3 G_5 G_8 M_{F1} M_{F2} D_0^{(s-u)} \quad (B.136)$$

$$C_{VLL}^{(s)} = -4G_1 G_3 G_5 G_7 \left(C_0^{(s-u)} + M_{F1}^2 D_0^{(s-u)} - 3D_0^{(s-u)} \right) \quad (B.137)$$

$$C_{VLR}^{(s)} = -4G_1 G_3 G_6 G_8 \left(C_0^{(s-u)} + M_{F1}^2 D_0^{(s-u)} \right) \quad (B.138)$$

$$C_{SLL}^{(t)} = -4G_2 G_3 G_5 G_8 M_{F1} M_{F2} D_0^{(s-u)} \quad (B.139)$$

$$C_{SLR}^{(t)} = -4G_2 G_3 G_6 G_7 M_{F1} M_{F2} D_0^{(s-u)} \quad (B.140)$$

$$C_{VLL}^{(t)} = 16G_1 G_3 G_5 G_7 D_0^{(s-u)} \quad (B.141)$$

$$C_{VLR}^{(t)} = 4G_1 G_3 G_6 G_8 D_0^{(s-u)} \quad (B.142)$$

$$C_{SLL}^{(u)} = -4G_2 G_4 G_5 G_7 M_{F1} M_{F2} D_0^{(s-u)} \quad (B.143)$$

$$C_{SLR}^{(u)} = -8G_2 G_3 G_5 G_8 D_0^{(s-u)} \quad (B.144)$$

$$C_{VLL}^{(u)} = 16G_1 G_3 G_5 G_7 D_0^{(s-u)} \quad (B.145)$$

$$C_{VLR}^{(u)} = 2G_1 G_4 G_5 G_8 M_{F1} M_{F2} D_0^{(s-u)} \quad (B.146)$$

$$C_{SLL}^{(v)} = 8G_2 G_3 G_6 G_7 M_{F1} M_{F2} D_0^{(v-x)} \quad (B.147)$$

$$C_{SLR}^{(v)} = 8G_2 G_3 G_5 G_8 \left(C_0^{(v-x)} + M_{V1}^2 D_0^{(v-x)} \right) \quad (B.148)$$

$$C_{VLL}^{(v)} = -4G_1 G_3 G_5 G_7 \left(C_0^{(v-x)} + M_{V1}^2 D_0^{(v-x)} - 3D_0^{(v-x)} \right) \quad (B.149)$$

$$C_{VLR}^{(v)} = 2G_1 G_3 G_6 G_8 M_{F1} M_{F2} D_0^{(v-x)} \quad (B.150)$$

$$C_{SLL}^{(w)} = 8G_1 G_3 G_6 G_8 M_{F1} M_{F2} D_0^{(v-x)} \quad (B.151)$$

$$C_{SLR}^{(w)} = 32G_1 G_3 G_5 G_7 D_0^{(v-x)} \quad (B.152)$$

$$C_{VLL}^{(w)} = -2G_2 G_3 G_6 G_7 M_{F1} M_{F2} D_0^{(v-x)} \quad (B.153)$$

$$C_{VLR}^{(w)} = 4G_2 G_3 G_5 G_8 D_0^{(v-x)} \quad (B.154)$$

$$C_{SLL}^{(x)} = -4G_1 G_4 G_5 G_8 M_{F1} M_{F2} D_0^{(v-x)} \quad (B.155)$$

$$C_{SLR}^{(x)} = -8G_1 G_3 G_5 G_7 \left(C_0^{(v-x)} + M_{V1}^2 D_0^{(v-x)} - 3D_0^{(v-x)} \right) \quad (B.156)$$

$$C_{VLL}^{(x)} = -2G_2 G_3 G_5 G_8 M_{F1} M_{F2} D_0^{(v-x)} \quad (B.157)$$

$$C_{VLR}^{(x)} = -4G_2 G_4 G_5 G_7 \left(C_0^{(v-x)} + M_{V1}^2 D_0^{(v-x)} \right) \quad (B.158)$$

The arguments of the loop functions for the different amplitudes are

$$D_X^{(a-c)} = D_X(M_{F1}^2, M_{F2}^2, M_{S1}^2, M_{S2}^2) \quad (B.159)$$

$$D_X^{(d-f)} = D_X(M_{F1}^2, M_{F2}^2, M_{S1}^2, M_{S2}^2) \quad (B.160)$$

$$C_X^{(g-i)} = C_X(\vec{0}_3, M_{F2}^2, M_V^2, M_S^2) \quad D_X^{(g-i)} = D_X(M_{F1}^2, M_{F2}^2, M_V^2, M_S^2) \quad (B.161)$$

$$C_X^{(j-l)} = C_X(\vec{0}_3, M_{F2}^2, M_S^2, M_V^2) \quad D_X^{(j-l)} = D_X(M_{F1}^2, M_{F2}^2, M_S^2, M_V^2) \quad (B.162)$$

$$C_X^{(m-o)} = C_X(\vec{0}_3, M_{F2}^2, M_{F1}^2, M_V^2) \quad D_X^{(m-o)} = D_X(M_{F2}^2, M_{F1}^2, M_S^2, M_V^2) \quad (B.163)$$

$$C_X^{(p-r)} = C_X(\vec{0}_3, M_{F2}^2, M_{F1}^2, M_S^2) \quad D_X^{(p-r)} = D_X(M_{F2}^2, M_{F1}^2, M_V^2, M_S^2) \quad (B.164)$$

$$C_X^{(s-u)} = C_X(\vec{0}_3, M_{F2}^2, M_{V1}^2, M_{V2}^2) \quad D_X^{(s-u)} = D_X(M_{F1}^2, M_{F2}^2, M_{V1}^2, M_{V2}^2) \quad (B.165)$$

$$C_X^{(v-x)} = C_X(\vec{0}_3, M_{F2}^2, M_{F1}^2, M_{V2}^2) \quad D_X^{(v-x)} = D_X(M_{F2}^2, M_{F1}^2, M_{V1}^2, M_{V2}^2) \quad (\text{B.166})$$

References

- [1] G. Aad *et al.* [ATLAS Collaboration], Phys. Lett. B **716**, 1 (2012) [arXiv:1207.7214 [hep-ex]].
- [2] S. Chatrchyan *et al.* [CMS Collaboration], Phys. Lett. B **716**, 30 (2012) [arXiv:1207.7235 [hep-ex]].
- [3] **ATLAS Collaboration** Collaboration, G. Aad *et al.*, “Search for squarks and gluinos with the ATLAS detector in final states with jets and missing transverse momentum using 4.7 fb⁻¹ of sqrt(s) = 7 TeV proton-proton collision data,” [arXiv:1208.0949 [hep-ex]]
- [4] **CMS Collaboration** Collaboration, S. Chatrchyan *et al.*, “Search for supersymmetry in hadronic final states using MT2 in *pp* collisions at sqrt(s) = 7 TeV,” JHEP **1210** (2012) 018, [arXiv:1207.1798 [hep-ex]]
- [5] **CMS Collaboration** Collaboration, “Search for supersymmetry in final states with missing transverse momentum and 0, 1, 2, or ≥ 3 b jets with CMS,”.
- [6] **CMS Collaboration** Collaboration, “Search for supersymmetry with the razor variables at CMS,”.
- [7] **CMS Collaboration** Collaboration, S. Chatrchyan *et al.*, “Search for new physics in the multijet and missing transverse momentum final state in proton-proton collisions at sqrt(s) = 7 TeV,” [arXiv:1207.1898 [hep-ex]]
- [8] E. Arganda and M. J. Herrero, Phys. Rev. D **73** (2006) 055003 [hep-ph/0510405].
- [9] A. Arbey, M. Battaglia, A. Djouadi and F. Mahmoudi, arXiv:1211.4004 [hep-ph]. M. W. Cahill-Rowley, J. L. Hewett, A. Ismail and T. G. Rizzo, arXiv:1211.1981 [hep-ph]. S. S. AbdusSalam, arXiv:1211.0999 [hep-ph]. H. Baer and J. List, arXiv:1205.6929 [hep-ph]. M. Carena, J. Lykken, S. Sekmen, N. R. Shah and C. E. M. Wagner, Phys. Rev. D **86**, 075025 (2012) [arXiv:1205.5903 [hep-ph]]. P. Bechtle, T. Bringmann, K. Desch, H. Dreiner, M. Hamer, C. Hensel, M. Kramer and N. Nguyen *et al.*, JHEP **1206**, 098 (2012) [arXiv:1204.4199 [hep-ph]]; O. Buchmueller, R. Cavanaugh, M. Citron, A. De Roeck, M. J. Dolan, J. R. Ellis, H. Flacher and S. Heinemeyer *et al.*, Eur. Phys. J. C **72** (2012) 2243 [arXiv:1207.7315 [hep-ph]].
- [10] L. J. Hall and M. Suzuki, Nucl. Phys. B **231** (1984) 419. B. C. Allanach, A. Dedes and H. K. Dreiner, Phys. Rev. D **69** (2004) 115002 [Erratum-ibid. D **72** (2005) 079902] [hep-ph/0309196]. H. K. Dreiner, In *Kane, G.L. (ed.): Perspectives on supersymmetry II* 565-583 [hep-ph/9707435]. G. Bhattacharyya, In *Tegernsee 1997, Beyond the desert 1997* 194-201 [hep-ph/9709395]. R. Barbier *et al.*, Phys. Rept. **420**, 1 (2005) [hep-ph/0406039].
- [11] H. K. Dreiner and T. Stefaniak, Phys. Rev. D **86** (2012) 055010 [arXiv:1201.5014 [hep-ph]]. H. K. Dreiner and G. G. Ross, Nucl. Phys. B **365** (1991) 597. M. Asano, K. Rolbiecki and K. Sakurai, arXiv:1209.5778 [hep-ph]. B. C. Allanach and B. Gripaios, JHEP **1205** (2012) 062 [arXiv:1202.6616 [hep-ph]]. H. K. Dreiner, S. Grab and T. Stefaniak, Phys. Rev. D **84** (2011) 035023 [arXiv:1102.3189 [hep-ph]].
- [12] H. Dreiner, M. Kramer and J. Tattersall, arXiv:1211.4981 [hep-ph]. H. K. Dreiner, M. Kramer and J. Tattersall, Europhys. Lett. **99** (2012) 61001 [arXiv:1207.1613 [hep-ph]]. J. F. Gunion and S. Mrenna, Phys. Rev. D **62** (2000) 015002 [hep-ph/9906270]. J. Alwall, M. -P. Le, M. Lisanti and J. G. Wacker, Phys. Rev. D **79** (2009) 015005 [arXiv:0809.3264 [hep-ph]]. T. J. LeCompte and S. P. Martin, Phys. Rev. D **84** (2011) 015004 [arXiv:1105.4304 [hep-ph]]. T. J. LeCompte and S. P. Martin, Phys. Rev. D **85** (2012) 035023 [arXiv:1111.6897 [hep-ph]].
- [13] U. Ellwanger, G. Espitalier-Noel and C. Hugonie, JHEP **1109**, 105 (2011) [arXiv:1107.2472 [hep-ph]]. L. J. Hall, D. Pinner and J. T. Ruderman, JHEP **1204** (2012) 131 [arXiv:1112.2703 [hep-ph]]. G. G. Ross and K. Schmidt-Hoberg, Nucl. Phys. B **862**, 710 (2012) [arXiv:1108.1284 [hep-ph]]. G. G. Ross, K. Schmidt-Hoberg and F. Staub, JHEP **1208**, 074 (2012) [arXiv:1205.1509 [hep-ph]].
- [14] D. Stockinger, J. Phys. G **34** (2007) R45 [hep-ph/0609168].
- [15] T. P. Cheng and L. F. Li, *Gauge Theory Of Elementary Particle Physics*, Oxford, Uk: Clarendon (1984) 536 P. (Oxford Science Publications)
- [16] M. Misiak and M. Steinhauser, Nucl. Phys. B **764** (2007) 62 [hep-ph/0609241]; M. Misiak, H. M. Asatrian, K. Bieri, M. Czakon, A. Czarnecki, T. Ewerth, A. Ferroglia and P. Gambino *et al.*, Phys. Rev. Lett. **98** (2007) 022002 [hep-ph/0609232]; T. Hurth, E. Lunghi and W. Porod, Nucl. Phys. B **704** (2005) 56 [hep-ph/0312260]; M. Misiak and M. Steinhauser, Nucl. Phys. B **683** (2004) 277 [hep-ph/0401041]; C. Bobeth, P. Gambino, M. Gorbahn and U. Haisch, JHEP **0404** (2004) 071 [hep-ph/0312090].
- [17] A. J. Buras, R. Girsbach, D. Guadagnoli and G. Isidori, arXiv:1208.0934 [hep-ph].
- [18] A. J. Buras, R. Fleischer, J. Girsbach and R. Kneijens, arXiv:1303.3820 [hep-ph].
- [19] RAaij *et al.* [LHCb Collaboration], arXiv:1211.2674 [Unknown].
- [20] P. Fayet, Nucl. Phys. B **90** (1975) 104. H. P. Nilles, M. Srednicki and D. Wyler, Phys. Lett. B **120** (1983) 346. J. R. Ellis, J. F. Gunion, H. E. Haber, L. Roszkowski and F. Zwirner, Phys. Rev. D **39** (1989) 844. U. Ellwanger, C. Hugonie and A. M. Teixeira, Phys. Rept. **496**, 1 (2010) [arXiv:0910.1785 [hep-ph]].
- [21] F. Mahmoudi, Comput. Phys. Commun. **180** (2009) 1579 [arXiv:0808.3144 [hep-ph]]. F. Mahmoudi, Comput. Phys. Commun. **178** (2008) 745 [arXiv:0710.2067 [hep-ph]].
- [22] A. Crivellin, J. Rosiek, P. H. Chankowski, A. Dedes, S. Jaeger and P. Tanedo, arXiv:1203.5023 [hep-ph]. J. Rosiek, P. Chankowski, A. Dedes, S. Jager and P. Tanedo, Comput. Phys. Commun. **181** (2010) 2180 [arXiv:1003.4260 [hep-ph]].
- [23] U. Ellwanger, J. F. Gunion and C. Hugonie, JHEP **0502**, 066 (2005) [arXiv:hep-ph/0406215]. U. Ellwanger and C. Hugonie, Comput. Phys. Commun. **177**, 399 (2007) [arXiv:hep-ph/0612134].
- [24] G. Belanger, F. Boudjema, A. Pukhov and A. Semenov, Comput. Phys. Commun. **176**, 367 (2007) [arXiv:hep-ph/0607059].
- [25] W. Porod and F. Staub, Comput. Phys. Commun. **183** (2012) 2458 [arXiv:1104.1573 [hep-ph]]. W. Porod, Comput. Phys. Commun. **153** (2003) 275 [hep-ph/0301101].

- [26] F. Staub, arXiv:1207.0906 [hep-ph]. F. Staub, Comput. Phys. Commun. **182** (2011) 808 [arXiv:1002.0840 [hep-ph]]. F. Staub, Comput. Phys. Commun. **181** (2010) 1077 [arXiv:0909.2863 [hep-ph]]. F. Staub, arXiv:0806.0538 [hep-ph].
- [27] T. Inami and C. S. Lim, Prog. Theor. Phys. **65** (1981) 297 [Erratum-ibid. **65** (1981) 1772].
- [28] G. Buchalla and A. J. Buras, Nucl. Phys. B **400** (1993) 225.
- [29] M. Misiak and J. Urban, Phys. Lett. B **451** (1999) 161 [hep-ph/9901278].
- [30] C. -S. Huang, W. Liao and Q. -S. Yan, Phys. Rev. D **59** (1999) 011701 [hep-ph/9803460]. K. S. Babu and C. F. Kolda, Phys. Rev. Lett. **84** (2000) 228 [hep-ph/9909476]. C. Bobeth, T. Ewerth, F. Kruger and J. Urban, Phys. Rev. D **64** (2001) 074014 [hep-ph/0104284].
- [31] A. Dedes, H. K. Dreiner and U. Nierste, Phys. Rev. Lett. **87** (2001) 251804 [hep-ph/0108037].
- [32] A. Dedes, J. Rosiek and P. Tanedo, Phys. Rev. D **79** (2009) 055006 [arXiv:0812.4320 [hep-ph]].
- [33] J. Laiho, E. Lunghi and R. S. Van de Water, Phys. Rev. D **81** (2010) 034503 [arXiv:0910.2928 [hep-ph]].
- [34] C. Davies, PoS LATTICE **2011** (2011) 019 [arXiv:1203.3862 [hep-lat]].
- [35] H. K. Dreiner, M. Kramer and B. O’Leary, Phys. Rev. D **75**, 114016 (2007) [hep-ph/0612278].
- [36] T. Hahn, Comput. Phys. Commun. **140** (2001) 418 [hep-ph/0012260]. T. Hahn, Nucl. Phys. Proc. Suppl. **89** (2000) 231 [hep-ph/0005029]. T. Hahn, Acta Phys. Polon. B **30** (1999) 3469 [hep-ph/9910227]. S. Agrawal, T. Hahn and E. Mirabella, J. Phys. Conf. Ser. **368**, 012054 (2012) [arXiv:1112.0124 [hep-ph]].
- [37] F. Staub, T. Ohl, W. Porod and C. Speckner, Comput. Phys. Commun. **183** (2012) 2165 [arXiv:1109.5147 [hep-ph]].
- [38] F. Mahmoudi, S. Heinemeyer, A. Arbey, A. Bharucha, T. Goto, T. Hahn, U. Haisch and S. Kraml *et al.*, Comput. Phys. Commun. **183**, 285 (2012) [arXiv:1008.0762 [hep-ph]].
- [39] P. Z. Skands, B. C. Allanach, H. Baer, C. Balazs, G. Belanger, F. Boudjema, A. Djouadi and R. Godbole *et al.*, JHEP **0407**, 036 (2004) [hep-ph/0311123]. B. C. Allanach, C. Balazs, G. Belanger, M. Bernhardt, F. Boudjema, D. Choudhury, K. Desch and U. Ellwanger *et al.*, Comput. Phys. Commun. **180** (2009) 8 [arXiv:0801.0045 [hep-ph]].
- [40] L. Hofer and W. Porod (In preparation)
- [41] C. Bobeth, A. J. Buras, F. Kruger and J. Urban, Nucl. Phys. B **630**, 87 (2002) [hep-ph/0112305].
- [42] H. Arason, D. J. Castano, B. Keszthelyi, S. Mikaelian, E. J. Piard, P. Ramond, B. D. Wright and , Phys. Rev. D **46**, 3945 (1992).
- [43] S. Khalil and A. Masiero, Phys. Lett. B **665** (2008) 374 [arXiv:0710.3525 [hep-ph]].
- [44] P. Fileviez Perez and S. Spinner, Phys. Rev. D **83** (2011) 035004 [arXiv:1005.4930 [hep-ph]].
- [45] B. O’Leary, W. Porod, and F. Staub, JHEP **1205**, 042 (2012) [arXiv:1112.4600 [hep-ph]].
- [46] A. Crivellin, L. Hofer and J. Rosiek, JHEP **1107**, 017 (2011) [arXiv:1103.4272 [hep-ph]].
- [47] S. P. Martin and M. T. Vaughn, Phys. Rev. D **50** (1994) 2282 [Erratum-ibid. D **78** (2008) 039903] [arXiv:hep-ph/9311340].
- [48] R. M. Fonseca, M. Malinsky, W. Porod and F. Staub, Nucl. Phys. B **854**, 28 (2012) [arXiv:1107.2670 [hep-ph]].
- [49] F. Lyonnet, I. Schienbein, F. Staub and A. Wingerter (work in preparation)
- [50] D. M. Pierce, J. A. Bagger, K. T. Matchev and R. j. Zhang, Nucl. Phys. B **491**, 3 (1997) [arXiv:hep-ph/9606211].